AIAA-2000-4027

EFFECTS OF ECLIPSE BOUNDARY CROSSINGS ON THE NUMERICAL INTEGRATION OF ORBIT TRAJECTORIES

J. Woodburn*

Analytical Graphics, Inc.

ABSTRACT

The integration of orbit trajectories requires a combination of force modeling, a formulation of the equations of motion and a numerical integration technique to be specified. While it is common to separate these components of the problem conceptually, certain cross dependencies must be considered in the implementation process. The inclusion of solar radiation pressure in the force model introduces such a cross dependency with the integration procedure when the satellite crosses boundaries between lighting domains. The formulation of the equations of motion influences this through the integration step size. The effects of shadow boundary crossing for a variety of combinations of shadow models, integration methods and equations of motion are seen to vary greatly between Low Earth Orbits (LEO) and Highly Eccentric Orbits (HEO). These effects have somewhat predictable trends for LEOs but these trends disappear and the magnitude of the errors increase significantly for HEOs. It is also shown that integration closure testing can mask errors introduced during the crossing of shadow boundaries in certain circumstances.

INTRODUCTION

The use of special perturbation methods is widely regarded as the most accurate means for computing orbit trajectories. A special perturbations method is comprised of three separate, but related parts: a model for the forces acting on the satellite, a formulation of the equations of motion and a numerical integration procedure. Each part may be fundamentally sound on its own, but the impact of the assumptions made in each part must be considered when the parts are combined to solve a particular problem.

One area where the interaction between the components of the special perturbations method is especially important is in the modeling of effects of solar radiation pressure. The important assumptions in this case are made in the modeling of the Earth's shadow. The most common models for the shadow of the Earth are the conical model and the dual cone model. Each of these models has hard boundaries across which the model changes in form. These changes result in a discontinuity in the second order derivative of the position in the case of a cylindrical model and in a discontinuity or near discontinuity in the third derivative of the position in the case of a dual cone model. The existence of these discontinuities due to the shadow models violates the assumption, made in the formulation of many numerical integration methods, that the accelerations are smooth and continuous. It should be noted that the true transition between sunlight and darkness does not have hard boundaries but is actually a very complicated phenomenon. Absorption and refraction of the radiation by the atmosphere as well as the apparent deformation of the solar disk as seen through the Earth's atmosphere influence the level of illumination[1]. While detailed models of these phenomena exist, the complexity and computational burden imposed by such sophisticated shadow models has inhibited their widespread application[2].

The effect of discontinuities in the simpler shadow models on the accuracy of the integrated trajectory is dependent upon how the integration method a steps across the boundary[2,3]. The variables in this case are the location of the discontinuity within the step and the number and location of force model evaluations performed during the step. In some sense, the errors resulting from the crossing of shadow boundaries may have a self-correcting effect due to the variation in the

* Chief Orbital Scientist, Analytical Graphics Inc., Senior Member

geometry of the crossings. The fact that the dynamics of the orbit prediction problem are highly non-linear, however, makes the possibility of relying on such an occurrence seem risky.

Lundberg *et al.* have devised an algorithm for correcting the errors resulting from the crossing of shadow boundaries for multi-step integrators[3]. This algorithm is an improvement of an algorithm originally devised by Hubbard and documented in the open literature by Anderle[4]. Lundberg also derived a method for determining the step size for a multi-step integrator using a fixed step size to minimize the errors due to crossing shadow boundaries[5]. The optimal step size is computed to avoid situations where the time between the closest integration node and the shadow remains fairly constant. In this situation, the numerical integration is in a form of resonance with the eclipsing of the satellite and the errors incurred during the crossings of the shadow boundaries are less likely to cancel out over time.

The formulation of the equations of motion can also have a significant effect on the errors incurred during the crossing of shadow boundaries. This is due to the influence of the equations of motion on the step size of the integrator.

DESCRIPTION OF INVESTIGATION

An investigation of the errors introduced into the numerical integration of orbit trajectories was performed by sampling the trajectory errors from combinations of three integration methods in conjunction with two formulations of the equations of motion for both cylindrical and dual cone shadow models. The reader should be aware that this investigation is only looking at the effects of integrating across shadow boundaries on the solution produced by a set of modeling options. There is no measure made against *truth* orbits nor are the models being evaluated for their effectiveness as part of an orbit determination algorithm.

Shadow Models

The two types of shadow models used in this investigation were the cylindrical model and the dual cone model. The cylindrical model, illustrated in Figure 1, assumes that the Sun is infinitely far away such that all light is coming from a direction parallel to the direction to the Sun. The shadow cast by the Earth may then be represented as a cylinder of infinite length. The acceleration due to solar radiation pressure is simply set to zero when the satellite crosses the boundary from sunlight to shadow. This model is seemingly simple to implement since the only piece of information required is the component of the satellite position vector orthogonal to the Sun direction. The term *seemingly* is used since this model actually presents some computational difficulties that will be discussed later.

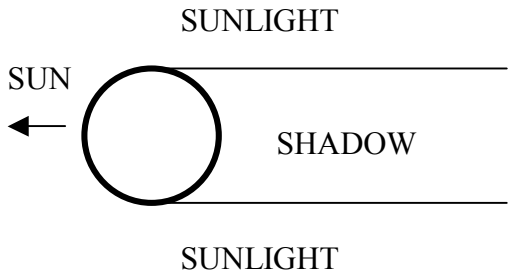

Figure 1. Cylindrical Shadow Model

The dual cone model establishes a region of partial illumination known as the penumbra region as shown in Figure 2. There are several common methods for computing the magnitude of the acceleration due to solar radiation pressure when the satellite is in the penumbra region. The method most consistent with the geometry of the model is to scale the acceleration of the satellite if it were in direct sunlight by the fractional area of the visible solar disk. Other methods include scaling the acceleration of the satellite if it were in direct sunlight based on a linear transition to full shadow and scaling the acceleration in full sunlight by one half. In this study, we scale the acceleration in full Sun by the fractional area of the solar disk.

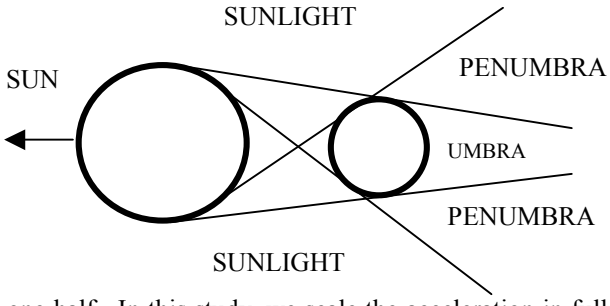

Figure 2. Dual Cone Shadow Model

Integration Methods

The integration methods investigated include two single step formulations and one multi-step formulation, as shown in Table 1. The Runge-Kutta-Fehlberg method is of order 7 and includes automatic step size control[6]. A new step size is computed for each step based on specified tolerance levels and error estimates from the prior step. The Bulirsch-Stoer single step method is investigated due to its increasing popularity and the fact the sampling of the force model across a step is very different from Runge-Kutta methods[7]. The Bulirsch-Stoer method also includes automatic step size control but can operate at varying order depending on the step size and error estimates. The step size is adjusted at each step based on specified error tolerances, error estimates from the prior step and an algorithm for maximizing the efficiency of the integration. The Stormer (predictor) Cowell (corrector) multi-step method is also a very widely used integrator and is sometimes referred to as the Gauss-Jackson method[8,9]. Stormer-Cowell is a Class II integrator for second order systems. The Stormer-Cowell formulation also requires either a fixed step size or a restart of the integrator when the step size is changed. For the purposes of this study, the step size was held constant when the Stormer-Cowell formulation was used. Each integration method is tested with both a dual cone and a cylindrical shadow model.

Table 1. Integration Methods

Method	Order	Type
Runge-Kutta-Fehlberg 7-8	7	Single step
Bulirsch-Stoer	N/A	Single step
Stormer-Cowell	12	Multi-step

Equations of Motion

Two formulations of the equations of motion were investigated. A Cowell formulation was used with all three integration methods. I will follow the distinction given by Vallado for referring to the second order equations describing the full accelerations on the satellite in cartesian coordinates as Cowell's formulation and the use of a finite differences based integration technique with Cowell's formulation as Cowell's method[9].

The second formulation of the equations of motion is the variation of parameters formulation (VOP) in universal variables as described by Herrick[10]. The VOP formulation contains first order differential equations and is therefore not suitable for use with the Stormer-Cowell integrator. The integration state was rectified at the completion of each integration step in the VOP formulation. A possible extension to the current test suite would be to use an Adams-Bashforth (predictor) Adams-Moulton (corrector) method with the VOP formulation. The step-wise rectification of the orbit would not be used in this case.

Initial Conditions

Two classes of orbits were studied, Low Earth Orbits (LEO) and Highly Eccentric Orbits (HEO). A set of initial conditions was selected for study from each class of orbit. Only the location of the ascending node was varied between elements of a set. The ascending node values are at five degree increments centered on the direction opposite to the direction to the Sun. The orbit elements selected for the study are given in Table 2. The LEO trajectories were integrated for one day and the HEO trajectories were integrated for one week so that both experience approximately the same number of shadow boundary crossings. The HEO trajectories were run with both a fixed time step and using time regularization with the Stormer-Cowell integrator. The fixed time steps for the Stormer-Cowell integrator were chosen based on accurate integration of the benchmark trajectories in the absence of shadow effects.

Table 2. Initial conditions

	LEO	HEO
Epoch	1 Jun 2000 00:00:00	1 Jun 2000 00:00:00
a (km)	7000.0	26561.743831
e	0.0	0.72
i (deg)	55.0	63.4
Ω (deg)	220.0->280.0	220.0->280.0

	LEO	HEO
ω (deg)	0.0	270.0
ν (deg)	0.0	90.0
C_p	2..0	2.0
A/M (m^2/kg)	0.02	0.02
SC Step Size (sec)	30.0	20.0

Benchmarks

To help identify that the differences in the results of numerical integration runs were caused by the crossing of shadow boundaries, each combination of initial conditions, integration method and formulation of equations of motion were run without a shadow model. In all cases the maximum difference between the trajectories for each initial condition set was less than one millimeter for the LEO cases. The maximum difference between the trajectories for each initial condition set was less than two centimeters for the HEO cases with one exception. The combination of the Runge-Kutta-Fehlberg integrator and the VOP formulation of the equations of motion produced trajectories which differed form the others by up to half a meter. It is believed that these differences are the result of inadequate error control during the adaptive step size selection. Differences between trajectories computed using shadow models can be considered to be due to the crossing of shadow boundaries if those differences are significantly larger than the differences in the benchmark trajectories.

Reference trajectories were also produced using each shadow model using the Runge-Kutta-Fehlberg and Bulirsch-Stoer integration methods. The integration in these cases was stopped and restarted at the boundaries of the shadow model to mitigate the effect of crossing the shadow boundary during an integration step. The validity of the results of these runs was verified by running the same trajectories at very small step sizes. A step size of 10 seconds was selected for the dual cone shadow model since the penumbra duration was approximately 9 seconds for the LEOs and between 8 and 18 seconds for the HEOs. Both integration methods sample the force model a number of times during an integration step which insures that the penumbra region will be sampled during a crossing. A step size of 1 second was used for the cylindrical shadow model since without stopping on the boundaries it is impossible to step across the boundary without having a significant discontinuity in the acceleration.

At this point, it is educational to refer back to the earlier comment about the simplicity of the cylindrical shadow model. While the shadow model is very simple to implement for the purpose of determining if the satellite is in shadow or not, it is deceptively difficult to stop and restart on the boundary. This difficulty arises from the fact that even when the time of the boundary crossing is solved for, numerical convergence and precision issues dictate that the spacecraft will be on one side or the other of the boundary. Since the goal of stopping and restarting is to prevent crossing the boundary during the step, it is necessary to supply additional logic to the force modeling to make sure that the correct lighting condition is used for the entire step approaching and the entire step away from the boundary. If this consistency is not enforced, the errors introduced into the numerical integration can actually be amplified.

TESTS

Prediction Tests

Sets of LEO and HEO trajectories were integrated forward for each combination of shadow model, integration method and formulation of the equations of motion without any mitigation of the effects of crossing the shadow boundaries. These trajectories were then compared with the reference solutions and the maximum positional error for each trajectory was recorded. The minimum, maximum and average of these positional errors was then determined across the set of trajectories for each combination. The results of these comparisons are given in Tables 3 and 4. When referring to Tables 3 and 4, it is important to note that the errors listed in the tables are those due to the numerical integration process, not relative to a *truth* orbit based on real data. The reference trajectories are computed using the same shadow model as the test where the integration was stopped and restarted at the shadow boundaries.

Table 3. LEO Prediction Errors

Combination	Minimum Error (m)	Maximum Error (m)	Average Error (m)
BS/COW/CYL	0.241	1.346	0.690
BS/COW/DC	0.124	1.213	0.480
BS/VOP/CYL	0.189	2.865	0.740
BS/VOP/DC	0.188	3.142	1.159
RK/COW/CYL	0.058	1.510	0.557
RK/COW/DC	0.055	0.591	0.237
RK/VOP/CYL	0.333	3.335	1.762
RK/VOP/DC	0.322	2.948	1.393
SC/COW/CYL	0.740	3.944	1.989
SC/COW/DC	0.319	2.045	1.151

Table 4. HEO Prediction Errors

Combination	Minimum Error (m)	Maximum Error (m)	Average Error (m)
BS/COW/CYL	1.605	46.292	14.069
BS/COW/DC	2.193	109.416	14.068
BS/VOP/CYL	3.786	33.601	12.043
BS/VOP/DC	3.316	55.676	16.219
RK/COW/CYL	1.513	33.441	10.880
RK/COW/DC	0.326	8.169	4.492
RK/VOP/CYL	11.910	118.365	55.493
RK/VOP/DC	6.509	83.263	45.542
SC/COW/CYL	4.152	54.926	19.780
SC/COW/DC	0.308	48.752	15.073
SC/COW^R/CYL	1.359	33.814	8.610
SC/COW^R/DC	1.293	25.584	5.641

The results for the LEO orbits shown in Table 3 show the general trends that might be expected based on a moderate understanding of the integration methods. Cases using the VOP formulation show larger errors than the corresponding cases using the Cowell formulation. This is to be expected since the VOP formulation allows for larger step sizes. The cylindrical shadow model usually introduces more error than the dual cone model. This seems reasonable due to the fact that the acceleration changes more drastically while crossing the boundary in the cylindrical model. Any sampling that occurs in the penumbra region of the dual cone model should serve to yield a more accurate step between shadow and sunlight. The exception to the trend for the shadow models occurs when the Bulirsch-Stoer method is used. Although a complete analysis of this behavior has not been performed, it may be related to the fact that the Bulirsch-Stoer method does not have a fixed number of force model evaluations per integration step. Instead, a sequence of possible sub-step samplings are performed until a suitable step is either produced or the step size is reduced and the process starts again. A more detailed study will be required to fully understand this interaction. The cases using the Stormer-Cowell integration method are also seen to be susceptible to the introduction of errors at shadow boundary crossings. This is expected since, as Lundberg points out, there is no information from within the predictor corrector step to indicate where within the step the crossing of the shadow boundary occurred[5].

The results for the HEO cases shown in Table 4 are much more difficult to understand. The trends based on the formulation of the equations of motion and the type of shadow model used are no longer apparent. Two additional cases have been added to the combinations used in the LEO tests. These cases use the Stormer-Cowell integration method with a time regularized Cowell formulation (COW^R) for the equations of motion. The only really identifiable trends are that the Runge-Kutta-Fehlberg and time regularized Stormer-Cowell cases appear to accumulate the least amount of error. The lack of predictability in the information

contained in Table 4 may be due to the fact that high eccentricity orbits are very sensitive to small perturbations.

Integration Closure Tests

A commonly used technique for evaluating the validity of a numerically integrated trajectory is the integration closure test. In this test, the trajectory is integrated forward and then the direction of the integration is reversed to return to the initial time. The final conditions are then compared to the initial conditions. The proper closure of the trajectory is a necessary condition for the integration to be considered accurate. The set of trajectories used in the prediction tests was subjected to closure testing with the exception of the time regularized cases. These tests were run in an attempt to determine the usefulness of the closure test for detecting the errors caused by crossing shadow boundaries. The results of these closure tests are shown in Tables 5 and 6.

Table 5. LEO Closure Errors

Combination	Minimum Error (m)	Maximum Error (m)	Average Error (m)
BS/COW/CYL	0.160	3.739	1.341
BS/COW/DC	0.165	1.775	1.121
BS/VOP/CYL	0.077	5.260	1.970
BS/VOP/DC	0.012	3.983	1.529
RK/COW/CYL	0.068	2.600	0.639
RK/COW/DC	0.025	0.968	0.406
RK/VOP/CYL	0.376	6.570	2.522
RK/VOP/DC	0.045	6.479	1.910
SC/COW/CYL	0.000	0.058	0.004
SC/COW/DC	0.000	0.219	0.017

Table 6. HEO Closure Errors

Combination	Minimum Error (m)	Maximum Error (m)	Average Error (m)
BS/COW/CYL	0.221	89.172	35.200
BS/COW/DC	0.521	129.504	35.270
BS/VOP/CYL	4.820	135.880	39.353
BS/VOP/DC	2.736	258.509	49.962
RK/COW/CYL	0.952	69.347	19.216
RK/COW/DC	0.876	32.592	9.652
RK/VOP/CYL	4.937	207.591	88.331
RK/VOP/DC	30.462	162.694	78.381
SC/COW/CYL	0.000	0.002	0.001
SC/COW/DC	0.000	0.001	0.001

The results in Tables 5 and 6 demonstrate clearly that while closure is a necessary condition for accurate numerical integration, it is not a sufficient condition. In almost all combinations, particular sets of initial conditions are integrated to closure levels which can be misleading in terms of the accuracy of the prediction. Especially relevant are the Stormer-Cowell results for the HEO orbits. The prediction errors in Tables 3 and 4 indicate that there are actually quite sizeable errors in the trajectory integration, but these errors are effectively masked by the integration closure test.

CONCLUSIONS

A preliminary investigation has shown that the unchecked crossing of shadow boundaries of both the cylindrical and the dual cone shadow models during the numerical integration process has been seen to introduce sizeable errors into the resulting trajectory. These errors were not measured against real data, but only against an implementation where the crossing of the boundaries during an integration step was avoided. The magnitude of the errors varies with the type of shadow model used and the numerical integration scheme and is influenced by the formulation of the

equations of motion via the integration step-size. While identifiable trends existed for the LEO cases, the HEO cases exhibited much more complicated behavior. In any case, it is apparent that for an orbit integration scheme to produce precise ephemeris, some means of mitigating these errors must be introduced. The simplest, but most computationally expensive, method is to reduce the maximum step size of the integration. A more effective means of mitigating the errors is to stop and restart the integrator on the boundaries. This can be computationally expensive in the case of multi-step integrators and non-trivial to program for single step integrators. A method, similar to that proposed by Hubbard and extended by Lundberg, but modified to work with other integration methods would probably be the best solution.

The possibility that errors in the integration of trajectories can go undetected by integration closure tests has also been demonstrated. More study is required to understand this behavior, but it is felt that this is an important point since many requirement specifications include such measures.

REFERENCES

1) Vokrouhlicky, D., Farinella, P., Mignard, F., "Solar Radiation Pressure Perturbations for Earth Satellites I: A complete theory including penumbra transitions," *Astronomy and Astrophysics*, 1993.

2) Hujsak, R.S., "Solar Pressure," Proceedings of the Artificial Satellite Theory Workshop, USNO, 1993.

3) Lundberg, J.B., Feulner, M.R., Abusali, P.A.M., Ho, C.S., "Improving the Numerical Integration Solution of Satellite Orbits in the Presense of Solar Radiation Pressure Using Modified Back Differences," AAS Paper 91-187, Presented at the AAS/AIAA Space Flight Mechanics Meeting, Feb. 1991.

4) Anderle, R.J., "Geodetic Analysis Through Numerical Integration," Proceedings of the International Symposium on the Use of Artificial Satellites for Geodesy and Geodynamics, Athens, Greece, 1973.

5) Lundberg, J.B., "Mitigation of Satellite Orbit Errors Resulting from the Numerical Integration Across Shadow Boundaries," AAS Paper 95-408, Presented at the AAS/AIAA Astrodynamics Specialist Conference, Halifax, Nova Scotia, August 1995.

6) Fehlberg, E., "Some Old and New Runge-Kutta Formulas with Stepsize Control and Their Error Coefficients," *Computing*, Vol. 34, 1985, pp 265-270.

7) Stoer, J., Bulirsch, R., *Introduction to Numerical Analysis*. New York: Springer-Verlag, 1980.

8) Maury, J.L., Segal, G.P., "Cowell Type Numerical Integration as Applied to Satellite Orbit Computation," Goddard Space Flight Center, NASA Technical Report TM-X-63542, X-553-69-46.

9) Vallado, David A., *Fundamentals of Astrodynamics and Applications*. New York: McGraw-Hill, 1997.

10) Herrick, Samuel, *Astrodynamics Volume II.* London: Van Nostrand Reinhold Company, 1972.